International Journal of the Physical Sciences Vol. 6(17), pp. 4287-4293, 2 September, 2011
Available online at http://www.academicjournals.org/IJPS
ISSN 1992 - 1950 ©2011 Academic Journals

Full Length Research Paper

Controlling crystallization and morphologies of monoclinic bismuth vanadate ($BiVO_4$) dendrite with enhanced photocatalytic activities

Haoyong Yin[1], Yongfei Sun[1], Dejun Shi[1], Xiaoxi Wang[1] and Ling Wang[2*]

[1]College of Materials and Environmental Engneering, Hangzhou Dianzi university, Hangzhou, 310018, P. R. China.
[2]Department of Chemistry, Zhejiang Sci-Tech University, Hangzhou, 310018, P. R. China.

Accepted 14 July 2011

The monoclinic $BiVO_4$ dendrites constructed by Bismuth vanadate ($BiVO_4$) branches with average diameters of about 100 nm have been successfully fabricated by Sodium dodecyl sulfate (SDS) assistant hydrothermal process. The monoclinic $BiVO_4$ dendrites were characterized by X-ray diffraction, scanning electron microscopy, Raman spectroscopy and transmission electron microscopy. The monoclinic $BiVO_4$ dendrites have uniform branches and the branches were transformed from the aggregated monoclinic $BiVO_4$ nanoparticles through the Ostwald ripening process. The monoclinic $BiVO_4$ dendrites show high efficient photocatalytic activities in decomposition of methyl orange.

Key words: Controlling crystallization, hierarchical structures, bismuth vanadate dendrites.

INTRODUCTION

Nowadays, the controllable synthesis of micro- and nano-scale materials with unique morphology and hierarchy has stimulated intensive interest due to their importance in basic scientific research and technological applications (Wang et al., 2006; Xia et al., 2003; Huang et al., 2006). Many efforts have been focused on the assembly of lower dimensional nanostructures into three-dimensional ordered superstructures, such as multipods, snowflakes and dendritic structures (Toprak et al., 2007; Ding et al., 2006; Wu et al., 2006). However, due to the difficulties in controlling the nucleation and growth processes, the construction of well - defined three - dimensional architectures with lower dimensional components is still a great challenge (Whitesides et al., 2002; Park et al., 2004; Xu et al., 2008). These hierarchical structures may endow them with morphology-dependant properties and imply their potential application in various fields. Therefore, further research is warranted to realize the advantages of them. Bismuth vanadate ($BiVO_4$), known for its ferroelasticity (Baker et al., 1991) ionic conductivity (Abraham et al., 1988) and pigmentation (Wood et al., 2004) has been extensively investigated recently. It has been used for a wide range of applications including gas sensors, posistors, solid-state electrolytes, positive electrode materials for lithium rechargeable batteries, and nontoxic yellow pigment for high-performance lead-free paints (Zhao et al., 2008) and recently proved to be a good photocatalyst for water splitting and pollutant decomposing under visible light irradiation (Ke et al., 2009; Shang et al., 2009). In the three structure types of bismuth vanadate–zircon tetragonal, scheelite monoclinic, and scheelite tetragonal, only the monoclinic scheelite $BiVO_4$ exhibits much higher visible-light photocatalytic activity over the other forms, giving rise to more attentions and wider researches (Zhang et al., 2006; Su et al., 2010, 2009). Besides crystalline form, the photocatalytic property of $BiVO_4$ also depends strongly on its microstructure, which is related to the synthesis method. To further improve the visible-light photocatalytic activity, a few submicron- or nanometer-sized $BiVO_4$ with various morphologoies have been prepared. Spindle-like $BiVO_4$ modified by polyaniline (PANI) (Shang et al., 2009) was synthesized via a sonochemical approach which shows efficient photocatalytic activity in the degradation of rhodamine (RhB) and phenol. Hydrothermal method was used to synthesize the bismuth vanadate ($BiVO_4$) nanosheets with good visible photocatalytic activities

*Corresponding author. E-mail: yhy@hdu.edu.cn. Tel: +86-591-87441126.

(Zhang et al., 2006). Pyramidal-shaped $BiVO_4$ nanowire arrays (Su et al., 2010) were vertically oriented to a fluorine doped tin oxide coated glass substrate by seed-mediated growth approach and show higher photocurrents in photoelectrochemical water splitting. The starlike $BiVO_4$ was also prepared using water/ethanol mixture as the solvent which exhibited high visible-light-driven photocatalytic efficiency (Sun et al., 2009). Considering the properties and applications are closely related to the microstructure and corresponding synthetic techniques and processes, it is of great importance to study the controllable synthesis of $BiVO_4$ with the desired crystalline phase and morphology.

Herein, we reported the preparation of monoclinic $BiVO_4$ dendrite by a simple hydrothermal method using SDS (Sodium dodecyl sulfate) to control its crystallization and morphologies. In this method SDS can both determine the crystalline phase and morphology of $BiOV_4$. Encouragingly, the as prepared monoclinic $BiVO_4$ dendrites exhibit high photocatalytic efficiency.

MATERIALS AND METHODS

All chemicals were analytical grade and were used as received without further purification. In a typical synthesis, 50 ml 0.13 M NH_4VO_3 solution was prepared by dissolving 6.5 mmol NH_4VO_3 into 50 ml $NH_3•H_2O$ solution (2 M). Meanwhile, 6.5 mmol $BiCl_3$ was dissolved in 50 ml of HNO_3 (4 M) which was added 5 mmol SDS in advance. Then NH_4VO_3 solution was slightly added into $BiCl_3$ solution under magnetic stirring. At last, the pH was adjusted by $NH_3•H_2O$ solution. This precursor solution was poured into a Teflon-lined stainless steel autoclave until 80% of the volume of the autoclave was occupied. The autoclave was heated at 160°C for 10 h at autogenous pressure. After the autoclave was cooled to room temperature, the precipitate was separated by filtration, washed with distilled water and absolute alcohol several times, and then dried at 60°C for 4 h. For comparison, another $BiVO_4$ sample was also prepared by the same procedure without adding SDS. The powder X-ray diffraction (XRD) patterns of as-synthesized samples were measured on a X-ray diffractometer (Bruker D8 ADVANCE) using monochromatized Cu Kα (λ = 0.15418 nm) radiation under 40 kV and 100 mA. The morphologies and microstructures of as-prepared samples were examined with scanning electron microscopy (SEM, JSM-6700F). Transmission electron microscopy (TEM) observations were carried out on a JEOL JEM-2100 instrument with accelerating voltage 200 kV in bright-field. The specimens used for TEM studies were dispersed in absolute ethanol by ultrasonic treatment. The sample was then dropped onto a copper grid coated with a holey carbon film and dried in air. The Raman spectra were analyzed using a German Bruker RFS 100/S Raman spectrometer. Brunauer–Emmett–Teller (BET) surface area was determined by nitrogen adsorption using a Micromeritics ASAP 2000 system.

Photocatalytic activities of the monoclinic $BiVO_4$ dendrites were evaluated by degradation of methyl orange under visible-light irradiation of a 500 W Xe lamp with a 420 nm cutoff filter. An aqueous $BiVO_4$ dispersion was prepared by adding 0.2 g of $BiVO_4$ powder into 100 ml of methyl orange solution (1 mg/L). The solution was magnetically stirred and irradiated by visible-light. After irradiation for a designated time, the dispersion was filtered to separate the $BiVO_4$ particles, and the methyl orange concentration of the filtrate was determined using the Lambda-35 UV-Vis spectrometer.

RESULTS AND DISCUSSION

The phase and composition of the as prepared products were investigated using XRD measurement (Figure 1). In Figure 1a, all diffraction peaks can be assigned to the monoclinic structure of $BiVO_4$ (JCPDS No. 14-0688) with space Group I2/a and no other peaks for impurities were detected. This observation is further confirmed by the splitting of the peaks at 2θ = 18.5, 35 and 46º, which is characteristic of the monoclinic structure of $BiVO_4$ (Tokunaga et al., 2001). The results show that the monoclinic scheelite $BiVO_4$ could be successfully synthesized by this simple hydrothermal method. Comparatively, for the samples synthesized without adding SDS in the mixed solution, the peaks were more complicated than that of the one with SDS at the same temperature (Figure 1b).There are tetragonal BiOCl phase coexisting with monoclinic $BiVO_4$ in the No SDS samples. The peaks in Figure 1b (marked with stars) fit well with the tetragonal BiOCl (JCPDS No. 85-0861). It suggested that the SDS did improve the crystallization of the $BiVO_4$. It is very helpful to the photocatalytic activity of $BiVO_4$.The morphologies of the monoclinic $BiVO_4$ dendrites prepared by SDS controlling procedures were revealed by SEM (Figure 2). The panoramic view in Figure 2a clearly demonstrates that the as-prepared products are almost entirely dendrite-like crystals with a length of 1 to 2 μm. As shown in Figure 2b, the individual dendrite has well defined branches with uniform diameters of about 100 nm and length of 100 to 500 nm, which demonstrates that the well-defined three-dimensional dendrites are successfully constructed with one dimensional branch components. The morphology and microstructure of monoclinic $BiVO_4$ dendrites were also investigated by transmission electron microscopy (Figure 3). Figure 3a shows a TEM image of part of monoclinic $BiVO_4$ dendrites. It also displays that the dendrites are comprised of 100 nm diameter branches which is consistent with the results of SEM images. Close observation of the samples revealed by HRTEM image (Figure 3b) shows that the surface of the monoclinic $BiVO_4$ dendrites branches is composed of a lot of $BiVO_4$ nano particles with the average diameter of about 8 nm. The clear lattice fringe (Figure 3c) indicates the high-crystallinity and single-crystalline nature of the branches. It can be measured that the d spacing is 0.468 nm, which agrees well with the lattice spacing (011) of monoclinic $BiVO_4$.

In order to investigate the effect of SDS on the morphology of $BiVO_4$ crystals, the samples prepared with the same procedure with different concentration of SDS were obtained. The SEM images (Figure 4) show that the morphologies can be greatly affected by the addition of SDS. Without SDS, the experimental system can only get the rod-like crystals with the diameter of about 100 nm (Figure 4a). After addition of 0.01 M SDS, the nanorods changed into shorter rods (Figure 4b). With 0.02 M SDS, the shorter rods began to aggregate (Figure 4c).

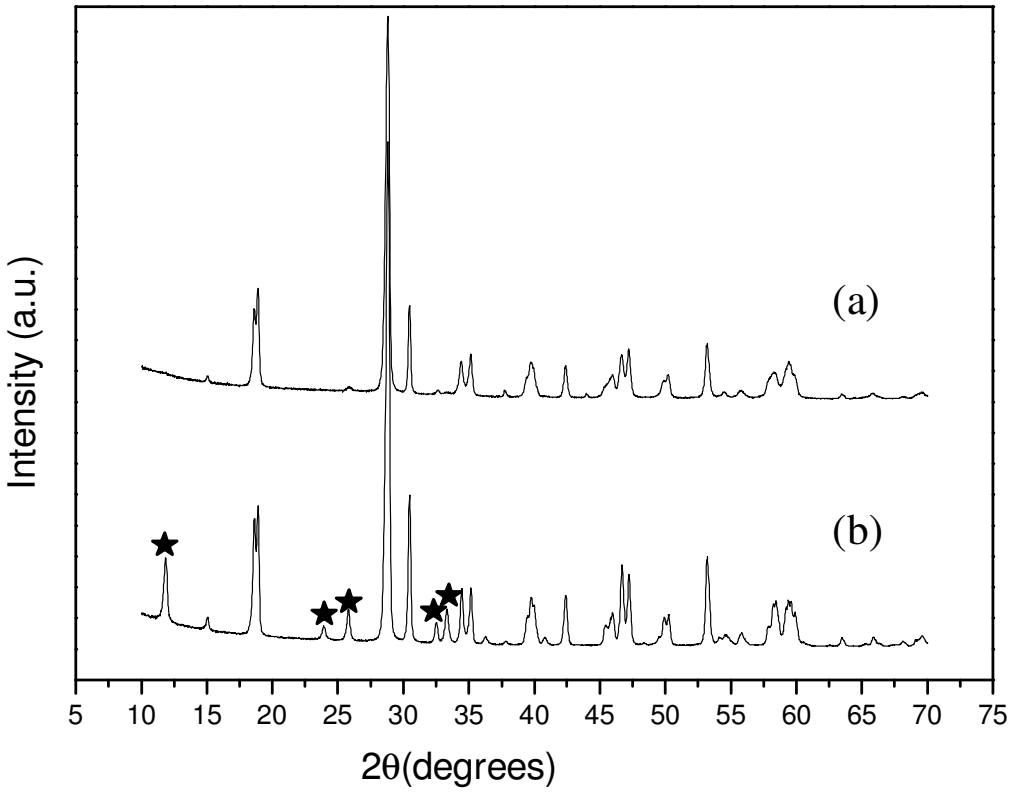

Figure 1. XRD patterns of the $BiVO_4$ synthesized under different conditions ((a) with SDS, (b) without SDS).

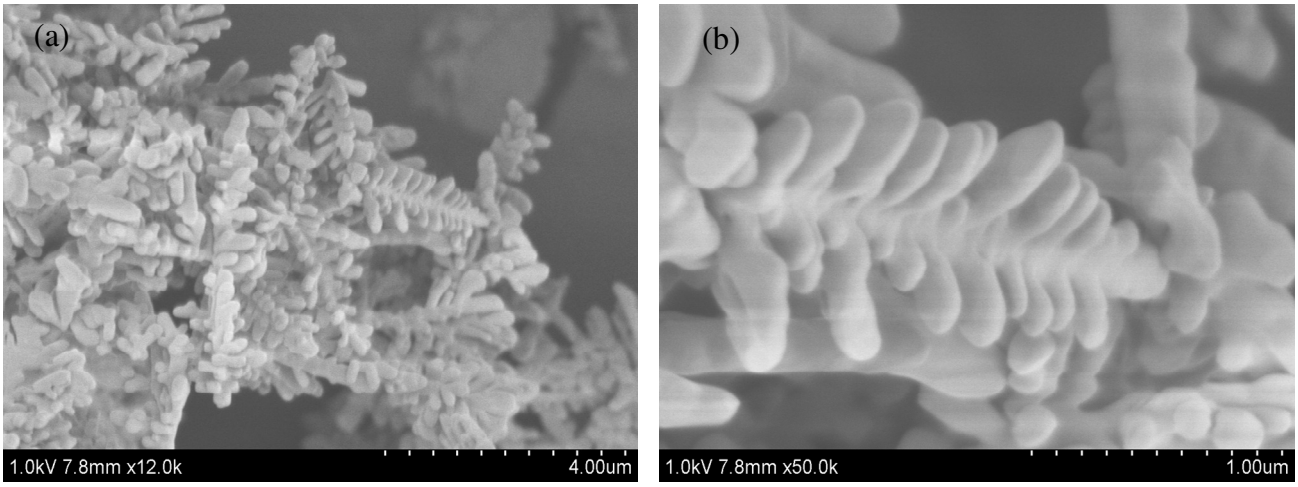

Figure 2. SEM image (a) and enlarged SEM image (b) of monoclinic $BiVO_4$ dendrites.

Continuously increasing the concentration of SDS to 0.03 M resulted in the appearing of small $BiVO_4$ dendrites (Figure 4d). When the concentration was increased into 0.05 M, the products are almost all dendrites $BiVO_4$ (Figure 4e). However, the over high concentration of SDS (0.07 M) can lead to the formation of $BiVO_4$ nanoparticles (Figure 4f). It can be drown from the results that SDS actually play an important role in controlling the morphologies of $BiVO_4$ dendrites. Combined with the results of XRD measurement (Figure 1b) the rod-like crystals mainly consist of monoclinic $BiVO_4$ and tetragonal BiOCl. This may be due to the formation process

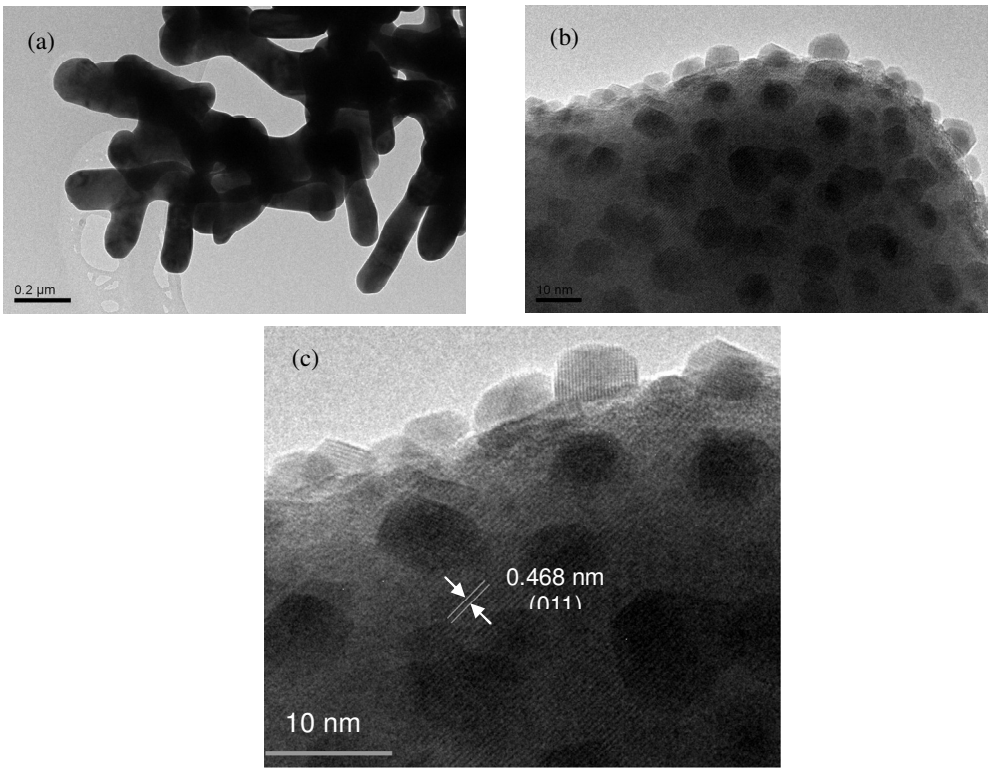

Figure 3. TEM image (a), HRTEM image (b) and enlarged HRTEM image (c) of monoclinic $BiVO_4$ dendrites.

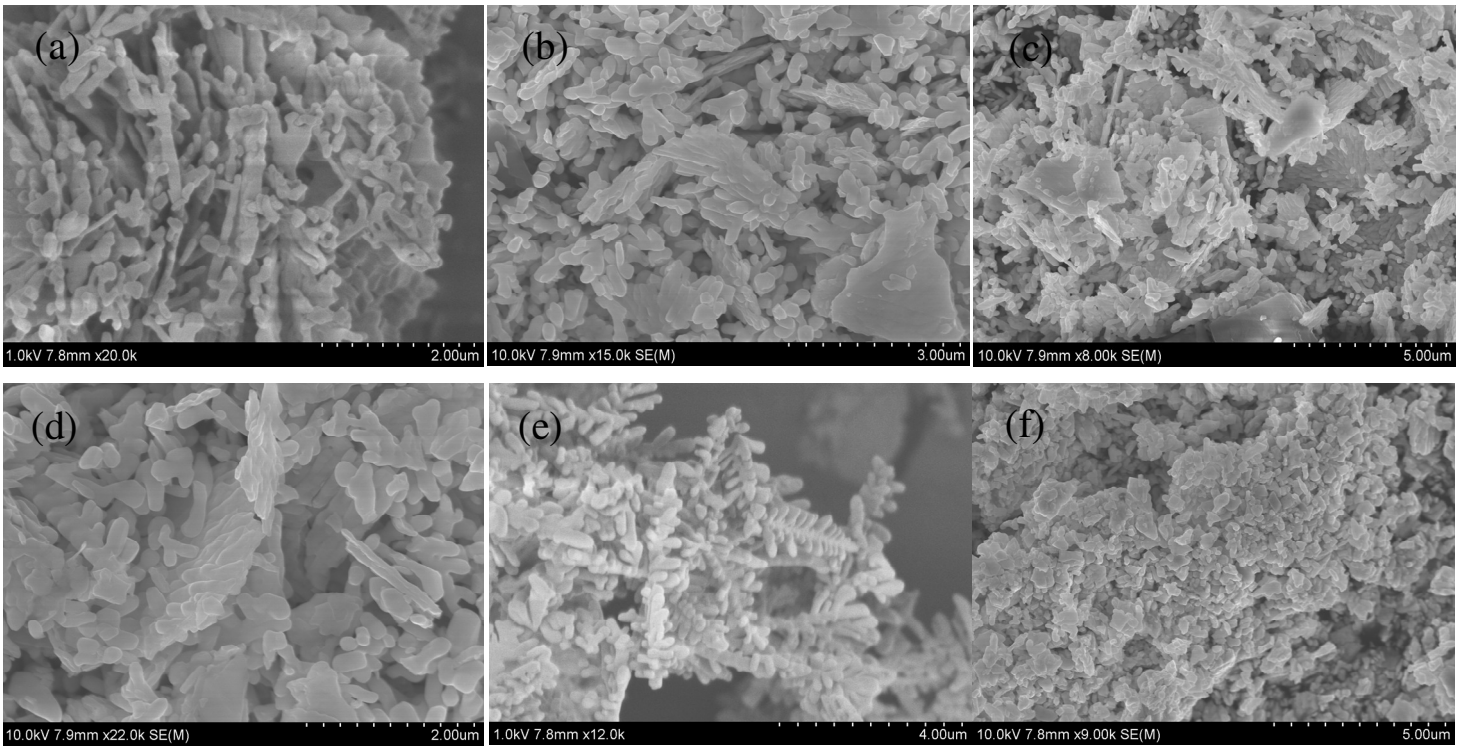

Figure 4. SEM image of $BiVO_4$ prepared with different concentration of SDS ((a) 0 M; (b) 0.01 M; (c) 0.02 M; (d) 0.03 M; (e) 0.05 M, and (f) 0.07 M).

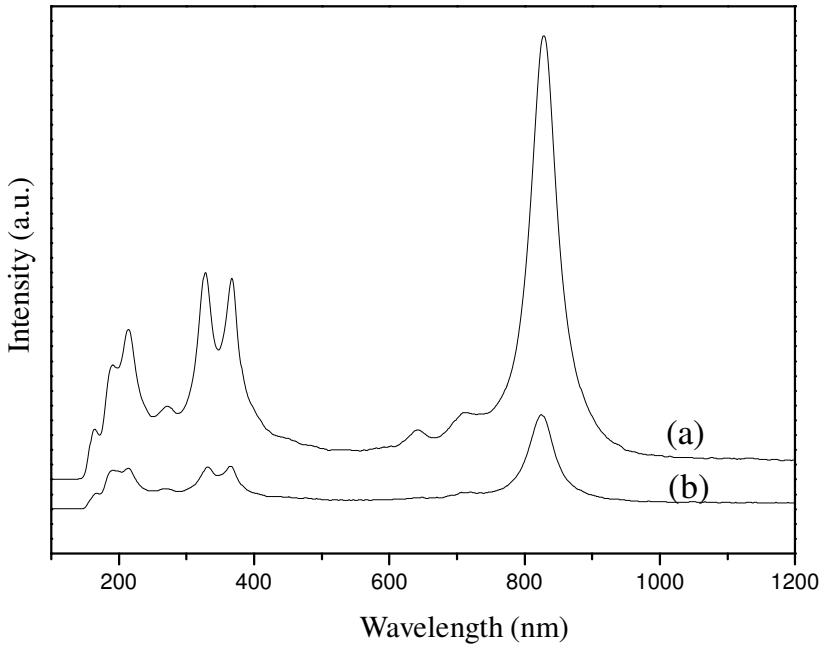

Figure 5. Raman scattering spectra of the monoclinic $BiVO_4$ dendrites (a) and $BiVO_4$ nanorods (b).

process of the monoclinic $BiVO_4$ during which some of $BiCl_3$ can hydrolyzes fast to BiOCl when dissolving in the solvent. Then BiOCl reacts with NH_4VO_3 to form monoclinic $BiVO_4$. In the SDS absent system, BiOCl can not entirely react with NH_4VO_3, therefore results in the mixed monoclinic $BiVO_4$ and tetragonal BiOCl phase nanorods. However, when adding SDS into the reaction system, the hydrolyzation of $BiCl_3$ may be inhibited, resulting in the direct reaction of Bi^{3+} with NH_4VO_3 to form pure monoclinic $BiVO_4$ dendrites. The XRD pattern in Figure 1a with pure monoclinic $BiVO_4$ peaks approved this reaction.

Raman spectra also verified the improved crystallization of monoclinic $BiVO_4$ dendrites. The Raman scattering spectra of the crystalline $BiVO_4$ samples were obtained in different experimental conditions (Figure 5). Raman bands at 330, 365 and 827cm^{-1} were observed in both monoclinic $BiVO_4$ dendrites and $BiVO_4$ nanorods. These Raman bands represented the typical vibration bands of monoclinic scheelite $BiVO_4$ and could be assigned to the asymmetric and symmetric deformation modes of VO_4^{3-} and the symmetric stretching mode of the V-O bond, respectively (Li et al., 2008). The Raman band at 210 cm^{-1} relates to the external mode of $BiVO_4$, which gives little structural information of the sample (Guo et al., 2010). However, the Raman bands of monoclinic $BiVO_4$ dendrites were slightly different from the $BiVO_4$ nanorods. The peaks of 710 and 640 cm^{-1} in Figure 5a, assigned to the asymmetric V-O_1 stretch (as1) and asymmetric V-O_2 stretch (as2) disappeared in Figure 5b which hints that the SDS does improve the crystallization of monoclinic $BiVO_4$ dendrites. The aforementioned results suggested that SDS played a vital role in the formation of monoclinic $BiVO_4$ dendrites. The whole process of SDS affecting the morphology of monoclinic $BiVO_4$ dendrites can be illustrated in Scheme 1. As an anionic surfactant, SDS can form pillar micelles in aqueous solution when the concentration is higher than its critical micelle concentration (CMC) (Step 1). Bi^{3+} will produce when $BiCl_3$ dissolve in the solution and each Bi^{3+} ion interacts electrostatically with sodium dodecyl sulfate ions to form bi-sodium dodecyl sulfate complexes, which then result in an ordered pillar mesostructure (Step 2). After addition of NH_3VO_4 the VO^{3-} can react with Bi^{3+} on the pillar mesostructure surface which then forms the monoclinic $BiVO_4$ nucleus on the surface (Step 3). Continuously reaction of Bi^{3+} and VO^{3-} will result in more monoclinic $BiVO_4$ nucleus and the congregation of the nucleus along energetically favorable directions on the pillar meso-structure surface (Step 4). These nucleus may eventually developed into the branches of the monoclinic $BiVO_4$ dendrites which can get a hint from the HRTEM of Figure 3b where there are still some undeveloped nucleus on the branch surface. During the hydrothermal process, the aggregated nucleus may undergo an Ostwald ripening process to form larger crystals, that is, the branches of the monoclinic $BiVO_4$ dendrites. Therefore, the well-defined monoclinic $BiVO_4$ dendrites with uniform branch components were successfully obtained by this simple hydrothermal SDS assistant method (Step 5). In order to investigate the effect of SDS on the photocatalytic activities of the as prepared products, the photocatalytic

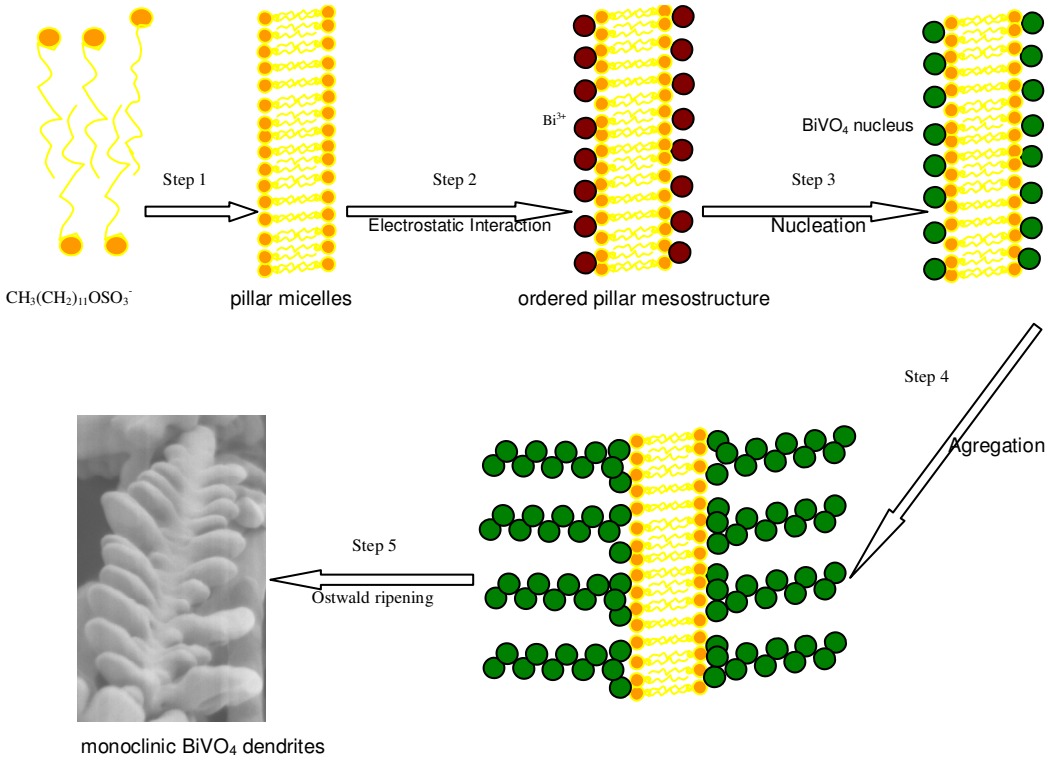

Scheme 1. Mechanism of the monoclinic $BiVO_4$ dendrites growth affected by SDS.

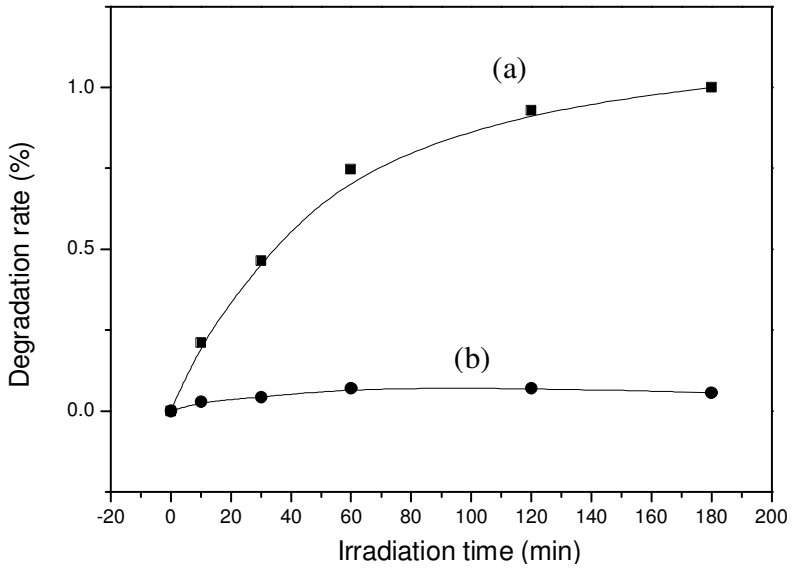

Figure 6. Degradation rates of MO on monoclinic $BiVO_4$ dendrites (a) and $BiVO_4$ nanorods (b) catalysts.

activities of monoclinic $BiVO_4$ dendrites and $BiVO_4$ nanorods were measured in liquid phase reactions. The decomposition of methyl orange in an aqueous solution was chosen as the photoreaction probe. The result shows that the degradation rates of monoclinic $BiVO_4$ dendrites is much higher than that of $BiVO_4$ nanorods (Figure 6) under the irradiation of visible light (400 nm < λ < 660 nm). Actually, there is almost no reaction when $BiVO_4$

nanorod was used as photocatalyst. This may be due to the fact that the hydrolyzation of $BiCl_3$ into BiOCl decreases the crystallization performance of $BiVO_4$ (Liu et al., 2010). Generally, the particles with well crystallinity can decrease the defects inside the crystals, which allows for the more efficient transfer of electron–hole pairs, generated inside the crystal, to the surface. Therefore, it is not surprising that the well-crystallized monoclinic $BiVO_4$ dendrites show the higher photocatalytic activity than that of $BiVO_4$ nanorod which might also be due to its unique morphologies and higher surface area (the surface area of $BiVO_4$ dendrites is 3.12 m^2/g which is higher than 1.26 m^2/g of $BiVO_4$ nanorods). It was reported that the photocatalytic property of monoclinic $BiVO_4$ is related to the distortion of the bi-O polyhedron (Zhang et al., 2006). The monoclinic $BiVO_4$ dendrites products are composed of branches with relatively large distortion of the unit cell due to the large surface strain which may be beneficial to its high photocatalytic activities.

Conclusion

In summary, the monoclinic $BiVO_4$ crystals with dendritic morphology have been synthesized by a facile hydrothermal process. SDS plays a decisive role in the formation of the monoclinic $BiVO_4$ dendrites. It can both enhance the crystallization and determine the morphology of the monoclinic $BiVO_4$ dendrites. In addition, the photocatalytic activities of monoclinic $BiVO_4$ dendrites are also much higher than that of $BiVO_4$ nanorods. These results may not only enrich the dendrite structures of inorganic compounds but also can provide a new surfactant assistant strategy to synthesize hierarchical structures materials.

ACKNOWLEDGMENTS

We acknowledge the financial support from the Qianjiang Personal Project of Zhejiang Province (no. 2009R10025), Zhejiang Provincial Natural Science Foundation (Y4110499) and the excellent Youth Foundation of the Key Laboratory of Advanced Textile Materials and Manufacturing Technology (Zhejiang Sci-Tech University), Ministry of Education.

REFERENCES

Abraham F, Debreuille-Gresse MF, Mairesse G, Nowogrocki G (1988). Phase Transitions and Ionic Conductivity in $Bi_4V_2O_{11}$ an Oxide with a Layered Structure. Solid State Ion. 28:529-532.

Baker TL, Faber KT, Readey DW (1991). Ferroelastic Toughening in Bismuth Vanadate. J. Am. Ceram. Soc., 74:1619-1623.

Ding YS, Shen XF, Gomez S, Luo H, Aindow M, Suib SL (2006). Hydrothermal Growth of Manganese Dioxide into Three-Dimensional Hierarchical Nanoarchitectures. Adv. Funct. Mater., 16: 549-555.

Guo YN, Yang X, Ma FY, Li KX, Xu L, Yuan X, Guo YH (2010). Additive-free controllable fabrication of bismuth vanadates and their photocatalytic activity toward dye degradation. Appl. Surf. Sci., 256:2215-2222.

Huang JX, Tao AR, Connor S, He RR, Yang PD (2006). A General Method for Assembling Single Colloidal Particle Lines. Nano Lett., 6:524-529.

Ke DN, Peng TY, Ma L, Cai P, Dai K (2009). Effects of Hydrothermal Temperature on the Microstructures of $BiVO_4$ and Its Photocatalytic O_2 Evolution Activity under Visible Light. Inorg. Chem., 48:4685-4691.

Li GS, Zhang DQ, Yu JC (2008). Ordered Mesoporous $BiVO_4$ through Nanocasting: A Superior Visible Light-Driven Photocatalyst. Chem Mater., 20:3983-3992.

Liu W, Yu Y, Cao L, Su Ge, Liu X, Zhang L, Wang Y (2010). Synthesis of monoclinic structured $BiVO_4$ spindly microtubes in deep eutectic solvent and their application for dye degradation. J. Hazard Mater., 181: 1102-1108.

Park S, Lim JH, Chung SW, Mirkin CA (2004). Self-assembly of mesoscopic metal-polymer amphiphiles. Sci., 303:348-351.

Shang M, Wang WZ, Sun SM, Ren J, Zhou L, Zhang L (2009). Efficient Visible Light-Induced Photocatalytic Degradation of Contaminant by Spindle-like PANI/$BiVO_4$. J. Phys. Chem. C., 113:20228-20233.

Sun SM, Wang WZ, Zhou L, Xu HL (2009). Efficient Methylene Blue Removal over Hydrothermally Synthesized Starlike $BiVO_4$. Ind. Eng. Chem. Res., 48:1735-1739.

Su JZ, Guo LJ, Yoriya S, Grimes CA (2010). Aqueous Growth of Pyramidal-Shaped $BiVO_4$ Nanowire Arrays and Structural Characterization: Application to Photoelectrochemical Water Splitting. Crystal. Growth & Design., 10:856-861.

Tokunaga S, Kato H, Kudo A (2001). Selective Preparation of Monoclinic and Tetragonal $BiVO_4$ with Scheelite Structure and Their Photocatalytic Properties. Chem. Mater., 13:4624-4628.

Toprak MS, McKenna BJ, Mikhaylova M, Waite JH, Stucky GD (2007). Spontaneous Assembly of Magnetic Microspheres. Adv. Mater., 19:1362-1368.

Wang ZL, Song JH (2006). Piezoelectric Nanogenerators Based on Zinc Oxide Nanowire Arrays. Sci,312:242-246.

Whitesides GM, Grzybowski B (2002). Self-Assembly at All Scales. Sci.,295:2418-2421.

Wood P, Glasser FP (2004). Preparation and Properties of Pigmentary Grade $BiVO_4$ Precipitate from aqueous solution. Ceramics Int., 6:875-882.

Wu ZC, Pan C, Yao ZY, Zhao QR, Xie Y (2006). Large-scale synthesis of single-crystal double-fold snowflake Cu_2S dendrites. Cryst. Growth. Des., 6:1717-1720.

Xia YN, Yang PD, Sun YG, Wu YY, Mayers B, Gates B, Yin YD, Kim F, Yan YQ (2003). One-Dimensional Nanostructures: Synthesis, Characterization, and Applications. Adv. Mater., 15:353-389.

Xu LP, Ding YS, Chen CH, Zhao LL, Rimkus C, Joesten R, Suib SL (2008). 3D Flowerlike α-Nickel Hydroxide with Enhanced Electrochemical Activity Synthesized by Microwave-Assisted Hydrothermal Method. Chem. Mater., 20:308-316.

Zhang L, Chen DR, Jiao XL (2006). Monoclinic Structured $BiVO_4$ Nanosheets: Hydrothermal Preparation, Formation Mechanism, and Coloristic and Photocatalytic Properties. J. Phys. Chem. B., 110:2668-2673

Zhao Y, Xie Y, Zhu X, Yan S, Wang SX (2008). Surfactant-Free Synthesis of Hyperbranched Monoclinic Bismuth Vanadate and its Applications in Photocatalysis, Gas Sensing, and Lithium-Ion Batteries. Chem.-Eur. J., 14:1601-1606.